Supplementary Information for

# $Th_3[Th_6(OH)_4O_4(H_2O)_6](SO_4)_{12}(H_2O)_{13}$: A Self-Assembled Microporous Open-Framework Thorium Sulfate

Jian Lin, Geng Bang Jin*, and L. Soderholm*

*Chemical Sciences and Engineering Division, Argonne National Laboratory, Argonne, Illinois 60439, United States*

**S1. Synthesis.** ***Caution!*** $^{232}Th$ is an α-emitting radioisotope, and standard precautions for handling radioactive materials should be followed when working with the quantities used in the syntheses that follow.

Amorphous Th hydroxide was precipitated from 1 mL solution of 1 M $Th(NO_3)_4$ in $H_2O$ with $NH_4OH$. The resulting white precipitate was washed several times with distilled water until the pH of the supernatant was near neutral. With vigorous stirring, the washed precipitate was dissolved in 1.875 mL 1 M $H_2SO_4$. Any undissolved precipitate was removed from the resulting solution with a 0.2 μm syringe filter, resulting in a clear $Th^{IV}$ solution with a pH of 2.50. For experiments at lower pH, 0−50 μL 1 M $H_2SO_4$ was added to this solution. Evaporation within the pH range ($2.40 < pH \leq 2.50$) yielded microcrystals of **1** ($Th_3[Th_6(OH)_4O_4(H_2O)_6](SO_4)_{12}(H_2O)_{13}\cdot xTh^{4+}\cdot ySO_4^{2-}\cdot nH_2O$) and **2** after approximately three days (Figure S1a). Evaporation of the solutions at lower pH values ($1.50 \leq pH < 2.40$) yielded $Th(SO_4)_2(H_2O)_7\cdot(H_2O)_2$ (**3**) (Figure S1c).[1] Co-formation of **1**, **2**, and **3** was observed at pH ~ 2.40 (Figure S1b). Compound **1** and **2** have the same crystal habit, making their yields difficult to estimate (Figure S1a, inset). Slight changes in pH of the initial solution affect the size and quality of the crystals that form. In addition, both **1** and **2** lose crystallinity rapidly after being removed from the mother liquor under ambient conditions. In contrast, compound **3** can be isolated as a pure phase and is stable under the same conditions.

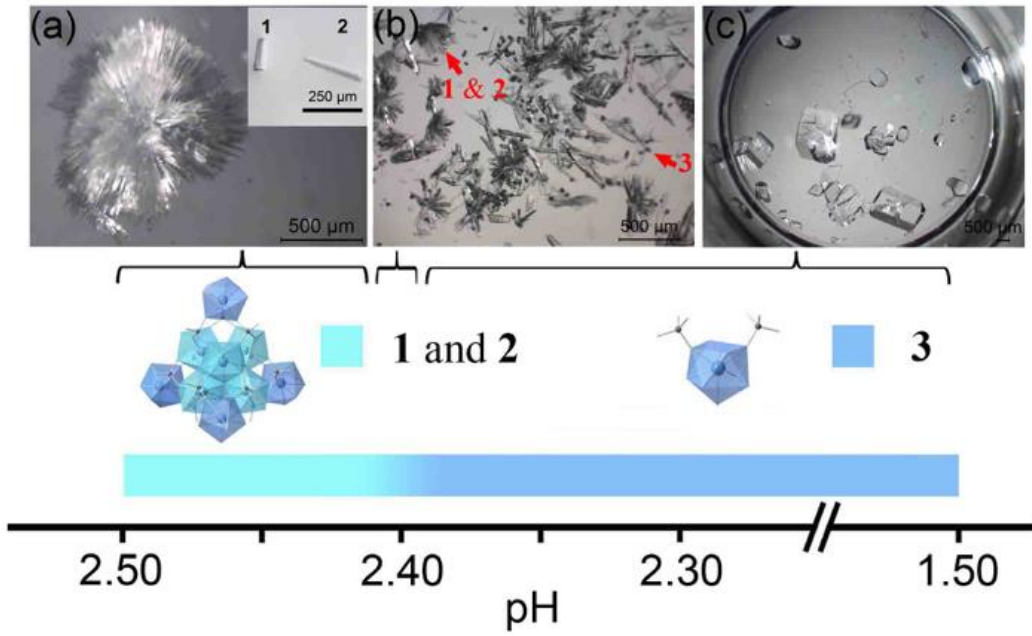


Figure S1. Composition diagram of the thorium-sulfate system as a function of solution pH showing the domains of three phases. (a) Clusters of microcrystal of **1** and **2** were isolated at 2.40 < pH ≤ 2.50 range; (b) Co-formation of crystals of **1**, **2**, and **3** was observed at pH ~ 2.40; (c) Crystals of compound **3** were isolated at 1.50 ≤ pH < 2.40 range.

**S2. X-ray structure determination.** Single-crystal X-ray diffraction data for **1**, **2**, and **3** were collected on a Bruker APEXII diffractometer equipped to produce monochromatized MoK$\alpha$ radiation ($\lambda$ = 0.71073 Å). The crystal-to-detector distance was 5.00 cm. Data were collected at 100 K with a scan rate of 0.3° in ω in groups of 600 frames at φ settings of 0°, 90°, 180°, and 270°. The exposure time was 30 s, 30 s, and 2 s per fame for structures **1**, **2**, and **3**, respectively. Intensity data collection, cell refinement, and data reduction were carried out with the use of the program *APEXII*.[2] *SAINT* software was used for data integration as well as Lorentz and polarization corrections.[3] Face-indexed absorption corrections, incident beam, and decay corrections were performed with the use of the program *SADABS*.[3] The structures were solved by direct methods using *SHELXS* and refined by full-matrix least-squares fitting on $F^2$ by *SHELXL-2014*.[4] Selected crystallographic information are listed in Table S1. Atomic coordinates and additional structural information are provided in the CIFs. For all structures, Th, S, and O atoms were assigned based on their electron densities and coordination environments.

***Structure of 1.*** The crystals of **1** are not stable at ambient conditions, losing crystallinity within hours after isolation from their mother liquor (Table S3). In contrast, there was no loss of crystallinity at 100 K, the temperature at which the data were collected. To verify this, an additional 60 frames were collected at $\varphi = 0°$ following the full dataset collection. Comparisons of the two sets of data revealed that reflection positions and intensities of the same frame ($\omega = 0°$, $\varphi = 0°$) remained unchanged, within error, after ~24 h of data collection.

All non-hydrogen atoms, except those in the void space of **1**, were refined anisotropically. During the refinement of **1**, a large area of residual electron density was located in the difference Fourier map with a short distance (~0.9 Å) to Th(9), suggesting disorder. The disorder was modeled with two sites, Th(9A)/Th(9B) constrained to a single-site sum. The two sites were initially refined to 0.624(2)/0.376(2) occupancy and were subsequently fixed during further refinement. Th(9) is coordinated by nine O atoms. Seven of them, including O(51), O(56), Ow(15), Ow(16), Ow(17), Ow(18), and Ow(19), have large displacement parameters compared to other O atoms (e.g. $U_{11}$ = 0.170(16) Å$^2$ for Ow(15) vs. $U_{11}$ = 0.060(6) Å$^2$ for Ow(10) coordinating Th(8)), suggesting disorder of these O atoms. Residual electron densities near O(51), O(56), Ow(18), and Ow(19) further suggest disorder. Modeling this disorder over two sites with 0.62/0.38 occupancy gave reasonable displacement parameters (Figure S2) and $Th^{IV}$–O bond distances (Table S2). Modeling Ow(15), Ow(16), and Ow(17) atoms into split sites was not attempted due to the absence of corresponding residual electron densities. Bond valance sums (BVS), calculated using measured bond distances, determined the valences of Th(9A) and Th(9B) at 4.24 and 3.99, respectively.[5]

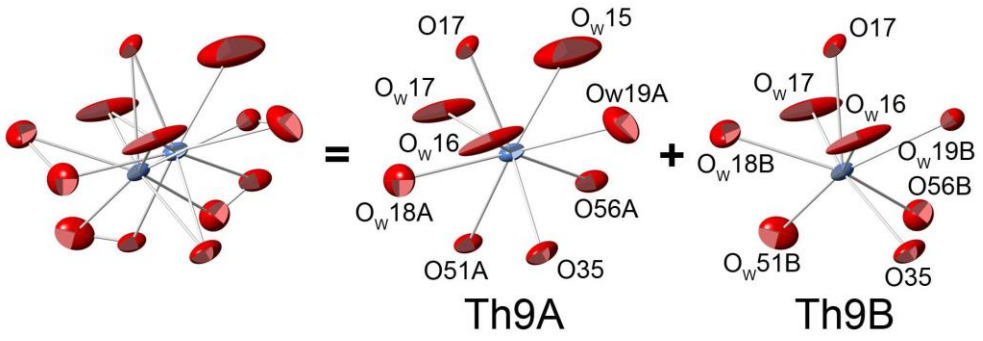


Figure S2. ORTEP representation of the coordination of Th(9) showing Th(9) is disordered over two sites with 62% occupancy for Th(9A) and 38% occupancy for Th(9B). The thermal ellipsoids are displayed at a probability of 50%. Th: dark blue, O: red.

X-ray diffraction data reveal significant electron density within the void space of **1**. Using the *SQUEEZE* routine within the *PLATON* software package, the electron count per cell was found to be 3747.2 $e^-$, corresponding to 468.4 $e^-$ per formula unit.[6] Approximately half of electron density within the voids can be modeled with $Th(10)^{4+}$, $S(13)O_4^{2-}$, and $H_2O$ moieties. The Th(10) position cannot be fully occupied, as the distances between two neighboring Th(10) atoms would amount to 2.653(3) Å. The occupancy of the Th(10) position was refined and determined to be 0.351(2). Each disordered Th is coordinated by seven O atoms, six from the hydration $H_2O$ and one from the $S(10)O_4^{2-}$ group. The Th(10)−O bond distances range from 2.37(3) Å to 2.63(3) Å, consistent with the other $Th^{IV}$−O bond distances in the structure. The S(13) atom has an occupancy of 0.39(1) with four coordinating O atoms in a tetrahedral geometry. Most $H_2O$ molecules in the voids are either disordered or partially occupied and their occupancies were refined freely. The remaining electron density in the voids is attributed to unresolved solvent water molecules and sulfate anions for balancing the charge of the occluded $Th^{IV}(10)$.

An additional diffraction dataset of **1** was collected on a different crystal from the one used for the refinement described above. The two crystals were synthesized as separate batches from solutions with the same pH (2.45). A comparison of the two structural refinements, reveals that their frameworks are invariant, $Th_3[Th_6(OH)_4O_4(H_2O)_6](SO_4)_{12}(H_2O)_{13}$, but the characters and the quantities of species occupying the void spaces are different. Only disordered water molecules were identified in the voids during the structural refinements of the second dataset. The authors acknowledge that the variations of the

species in the void space may result in charge-balance issues for the compound, but have found no evidence that this affects the charge-neutrality and structure of the framework.

***Structure of 2.*** Similar to **1**, the crystals of **2** undergo loss of crystallinity at ambient conditions upon removal from the mother liquor, but they are stable at 100 K (Table S3). Numerous crystals of **2** were isolated and examined. Unfortunately they are all severely twinned, and the final refinements of the structural model are less than satisfactory. We only provide the unit cell parameters and discuss some general atomic connectivity aspects of **2**. During the structural refinements of **2**, sixteen crystallographically independent Th and eighteen unique S atoms can be localized unambiguously in the difference Fourier map. From the sixteen Th atoms, two hexanuclear Th cores were identified. The Th−Th interatomic distances within the cores range from 3.944(4) Å to 3.966(3) Å, in good agreement with those refined in **1**. The remaining four Th atoms present as monomers with closest Th−Th distances of ~ 6 Å. These Th−Th distances suggest the presence of both hexanuclear cores and monomers in **2**.

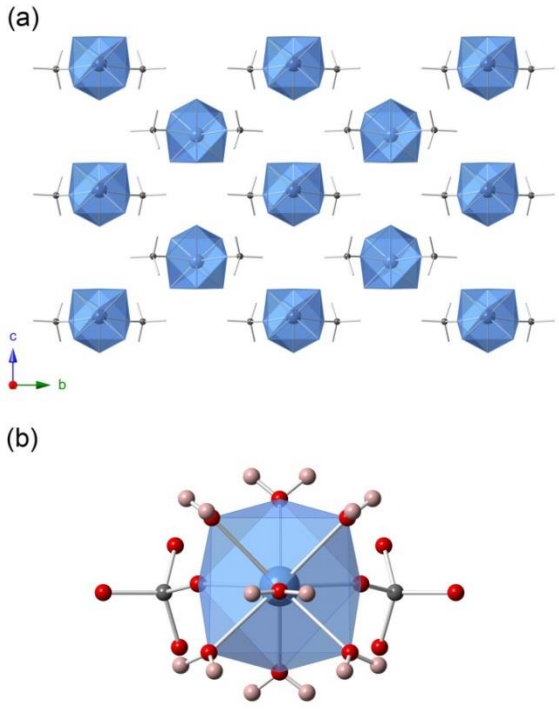


Figure S3. Illustration of **3** showing (a) its topology built from $Th(SO_4)_2(H_2O)_7$ monomers and (b) the local coordination environment of Th. Hydration water and hydrogen atoms have been omitted for clarity in (a). Th: dark blue, O: red, and H: pink.

***Structure of 3.*** For **3**, all the non-hydrogen atoms were refined anisotropically and all the hydrogen atoms were located in the Fourier maps. Compound **3** has been previously reported, with detailed structural information available in the literature.[1, 7] The structure of **3** is based on discrete $Th(SO_4)_2(H_2O)_7$ monomers built from one crystallographically independent Th center, one $SO_4^{2-}$ group, and five crystallographically unique water molecules (Figure S3). The Th center is coordinated by nine O atoms in a monocapped square antiprism

geometry within which two O atoms are from monodentate $SO_4^{2-}$ anions and seven O atoms are from water molecules.

**S1.3 Raman Spectroscopy.** Raman spectra of **1**, **2**, and **3** single-crystals were collected on a Renishaw inVia Raman Microscope with an excitation line of 532 nm at 10−50% laser power depending on the samples. Due to the radiological hazards associated with Th, each sample was placed on a glass drop-slide covered with a transparent coverslip, which was sealed to the slide using an epoxy sealant. Each spectrum consists of the summation of 50 acquisitions. As shown in Figure S4, the Raman spectra of **1**, **2**, and **3** are dominated by strong sulfate stretching and bending modes in the region of 1000−1200 $cm^{-1}$ and 420−660 $cm^{-1}$, respectively.[8] Similar vibration bands have been observed in other Th sulfate compounds.[1, 9] For example, the Raman spectra of $Th_3(SO_4)_6(H_2O)_6 \cdot H_2O$, shows the symmetric stretching mode of sulfate with an intense grouping of bands near 1060 $cm^{-1}$, and two weaker bending vibration bands at 650 and 450 $cm^{-1}$, respectively.[9] The Raman spectrum of **2** is comparatively closer to that of **1** than **3**. This is consistent with the structural refinements, which indicate similar structural motifs shared by **1** and **2** but not **3**. The spectra of **1** and **2** are similarly indicative of sulfate with symmetric stretching band centered at ~1030 $cm^{-1}$. Two weaker groupings of bands appear at ~460 $cm^{-1}$ and ~630 $cm^{-1}$, which can be assigned to the bending vibration modes of sulfate. The bands from 1100 $cm^{-1}$ to 1200 $cm^{-1}$ correspond to the anti-symmetric stretching modes. Although differences in the spectra of **1** and **2** could arise from different sulfate binding modes, the lack

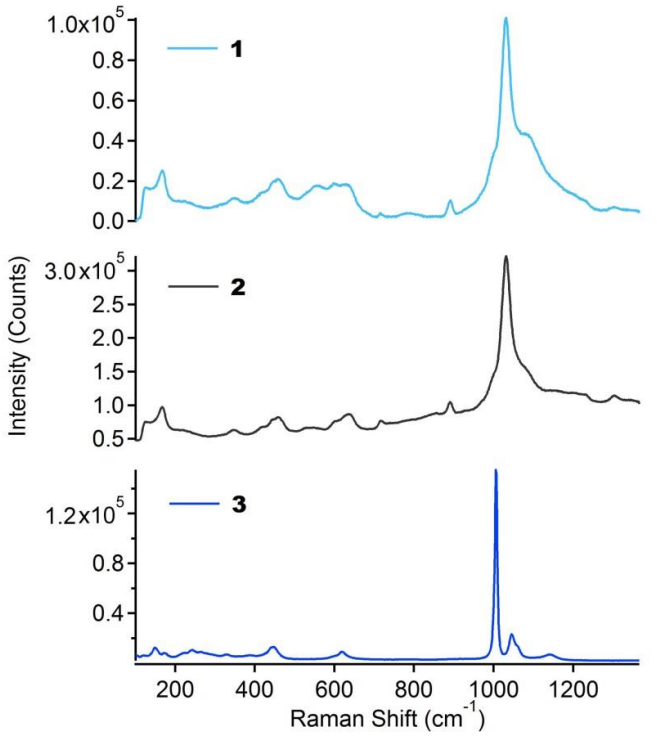


Figure S4. Raman spectra of **1**, **2**, and **3** over 100 – 1366 $cm^{-1}$.

of detailed structural information for **2** vitiates this conclusion. For compound **3**, the strongest peak corresponds to the symmetric stretching band centered at 1006 $cm^{-1}$, which is sharper than those in **1** and **2**. Vibrational bands corresponding to the bending modes of sulfate appear at ~450 $cm^{-1}$ and ~620 $cm^{-1}$. The characters and frequencies of these bands appear to be structurally related. There is only one crystallographically independent sulfate in the structure of **3** with a terminal-monodentate ($\eta_1$) coordination mode. In comparison, there are multiple crystallographically unique bridging ($\mu_3$ and $\mu_4$) sulfates in the structures of **1** and $Th_3(SO_4)_6(H_2O)_6 \cdot H_2O$.[9] The inclusion of these different sulfate units in the latter structures may contribute to the complex splitting and broadening of their vibrational bands.

Table S1. Crystallographic data and structure refinements for **1** (1st dataset), **2**, and **3**.

| | **1** | **2** | **3** |
|---|---|---|---|
| Empirical formula | $O_{99.23}S_{12.38}Th_{9.35}$ | ? | $H_{18}O_{17}S_2Th$ |
| Formula weight | 4154.37 [a] | ? | 586.30 |
| Crystal size (mm) | 0.056 × 0.062 × 0.126 | 0.060 × 0.103 × 0.227 | 0.485 × 0.145 × 0.116 |
| Colour | Colourless | Colourless | Colourless |
| Habit | Acicular | Acicular | Tabular or prismatic |
| Space group | *C*2/*c* (No. 15) | $P\bar{1}$ (No. 2) | $P2_1/m$ (No. 11) |
| *a* (Å) | 40.8076(18) | 17.533(7) | 7.2273(3) |
| *b* (Å) | 20.3710(9) | 20.513(8) | 12.1579(4) |
| *c* (Å) | 29.8948(13) | 29.977(12) | 7.9941(3) |
| $\alpha$ (º) | 90 | 90.023(5) | 90 |
| $\beta$ (º) | 109.9629(6) | 97.072(5) | 98.287 |
| $\gamma$ (º) | 90 | 114.773(5) | 90 |
| *V* (Å$^3$) | 23358.1(18) | 9699(7) | 695.10(5) |
| *Z* | 8 | ? | 2 |
| $\lambda$ (Å) | 0.71073 | 0.71073 | 0.71073 |
| T (K) | 100 | 100 | 100 |
| Maximum 2θ (deg.) | 27.544 | ? | 27.547 |
| $\rho_{calcd}$ (g·cm$^{-3}$) | 2.362 [a] | ? | 2.801 |
| $\mu$ (mm$^{-1}$) | 12.186 | ? | 11.114 |
| Tot. reflcns | 152847 | 69424 | 9177 |
| Unique reflcns | 26785 | 41630 | 1681 |
| R(int) | 0.0491 | 0.1059 | 0.0297 |
| GOF on $F^2$ | 1.049 | ? | 1.199 |
| R(F) [b] | 0.0412 | ? | 0.0127 |
| $R_w$ ($F_o^2$) [c] | 0.1159 | ? | 0.0313 |

[a] The formula weight and density given for compounds **1** are calculated without hydrogen. [b] $R(F) = \Sigma||F_o| - |F_c||/\Sigma|F_o|$ for $F_o^2 > 2\sigma(F_o^2)$. [c] $R_w(F_o^2) = \{\Sigma[w(F_o^2 - F_c^2)^2]/\Sigma wF_o^4\}^{1/2}$.

Table S2. Selected interatomic distances for **1**.

| **Assignment** | **Th(1)** | **Bond Distance (Å)** | **Th(2)** | **Bond Distance (Å)** | **Th(3)** | **Bond Distance (Å)** |
|---|---|---|---|---|---|---|
| Th···Th | Th1···Th2 | 3.9438 (5) | Th2···Th1 | 3.9438 (5) | Th3···Th1 | 3.9438 (5) |
| | Th1···Th3 | 3.9438 (5) | Th2···Th3 | 3.9524 (5) | Th3···Th2 | 3.9524 (5) |
| | Th1···Th4 | 3.9678 (4) | Th2···Th6 | 3.9579 (4) | Th3···Th5 | 3.9542 (4) |
| $\mu_3$-$O^{2-}$ | Th1−O1 | 2.336 (6) | Th2−O2 | 2.308 (6) | Th3−O2 | 2.320 (6) |
| | Th1−O2 | 2.299 (6) | Th2−O3 | 2.325 (6) | Th3−O4 | 2.311 (6) |
| $\mu_3$-$OH^-$ | Th1−O5 | 2.529 (6) | Th2−O5 | 2.508 (6) | Th3−O6 | 2.519 (6) |
| | Th1−O6 | 2.501 (6) | Th2−O7 | 2.491 (6) | Th3−O7 | 2.490 (6) |
| $H_2O$ | Th1−OW1 | 2.681 (6) | Th2−OW2 | 2.717 (8) | Th3−OW3 | 2.666 (7) |
| $-OSO_3^{2-}$ | Th1−O9 | 2.467 (6) | Th2−O21 | 2.456 (6) | Th3−O13 | 2.456 (6) |
| | Th1−O18 | 2.502 (5) | Th2−O29 | 2.493 (6) | Th3−O22 | 2.480 (6) |
| | Th1−O15 | 2.466 (6) | Th2−O46 | 2.472 (7) | Th3−O49i | 2.489 (6) |
| | Th1−O31 | 2.485 (6) | Th2−O41 | 2.485 (7) | Th3−O53i | 2.501 (7) |
| **Assignment** | **Th(4)** | **Bond Distance (Å)** | **Th(5)** | **Bond Distance (Å)** | **Th(6)** | **Bond Distance (Å)** |
| Th···Th | Th4···Th1 | 3.9678 (4) | Th5···Th3 | 3.9542 (4) | Th6···Th2 | 3.9579 (4) |
| | Th4···Th5 | 3.9541 (5) | Th5···Th4 | 3.9541 (5) | Th6···Th4 | 3.9520 (4) |
| | Th4···Th6 | 3.9520 (4) | Th5···Th6 | 3.9502 (5) | Th6···Th5 | 3.9502 (5) |
| $\mu_3$-$O^{2-}$ | Th4−O1 | 2.327 (6) | Th5−O3 | 2.309 (6) | Th6−O1 | 2.309 (6) |
| | Th4−O4 | 2.318 (6) | Th5−O4 | 2.306 (6) | Th6−O3 | 2.317 (6) |
| $\mu_3$-$OH^-$ | Th4−O6 | 2.507 (6) | Th5−O7 | 2.525 (6) | Th6−O5 | 2.488 (6) |
| | Th4−O8 | 2.522 (6) | Th5−O8 | 2.492 (6) | Th6−O8 | 2.485 (6) |
| $H_2O$ | Th4−OW4 | 2.749 (8) | Th5−OW5 | 2.686 (7) | Th6−OW6 | 2.726 (6) |
| $-OSO_3^{2-}$ | Th4−O10 | 2.475 (7) | Th−O34 | 2.474 (7) | Th6−O19 | 2.510 (6) |
| | Th4−O25 | 2.439 (6) | Th5−O38 | 2.483 (7) | Th6−O26 | 2.452 (7) |
| | Th4−O33 | 2.463 (7) | Th5−O42 | 2.489 (7) | Th6−O37 | 2.479 (6) |
| | Th4−O54i | 2.433 (7) | Th5−O50i | 2.460 (7) | Th6−O45 | 2.509 (6) |
| **Assignment** | **Th(7)** | **Bond Distance (Å)** | **Th(8)** | **Bond Distance (Å)** | **Th(9)** | **Bond Distance (Å)** |
| $-OSO_3^{2-}$ | Th7−O11ii | 2.398 (6) | Th8−O40iii | 2.429 (10) | Th9A−O17 | 2.371 (6) |
| | Th7−O14 | 2.371 (6) | Th8−O43iii | 2.362 (8) | Th9A−O35iv | 2.428 (7) |
| | Th7−O20ii | 2.469 (6) | Th8−O44 | 2.386 (8) | Th9A−O51A | 2.390 (10) |
| | Th7−O23 | 2.432 (6) | Th8−O48iii | 2.383 (9) | Th9A−O56A | 2.338 (12) |
| | Th7−O28ii | 2.340 (8) | | | Th9B−O17 | 2.552 (6) |
| | Th7−O30 | 2.365 (6) | | | Th9B−O35iv | 2.297 (7) |
| | | | | | Th9B−O51B | 2.37 (2) |
| | | | | | Th9B−O56B | 2.40 (2) |
| $H_2O$ | Th7−OW7 | 2.469 (7) | Th8−OW10 | 2.433 (10) | Th9A−OW15 | 2.629 (15) |
| | Th7−OW8 | 2.509 (9) | Th8−OW11 | 2.464 (10) | Th9A−OW16 | 2.609 (9) |
| | Th7−OW9 | 2.561 (9) | Th8−OW12 | 2.571 (10) | Th9A−OW17 | 2.362 (9) |
| | | | Th8−OW13 | 2.512 (11) | Th9A−OW18A | 2.468 (13) |
| | | | Th8−OW14 | 2.447 (11) | Th9A−OW19A | 2.525 (17) |
| | | | | | Th9B−OW16 | 2.403 (8) |
| | | | | | Th9B−OW17 | 2.444 (8) |
| | | | | | Th9B−OW18B | 2.49 (2) |

| | | | |
|---|---|---|---|
| | | | Th9B−OW19B 2.50 (2) |

Symmetry codes: (i) x, −y+1, z−1/2; (ii) −x+1/2, y+1/2, −z+1/2; (iii) −x, −y+1, −z; (iv) x, −y+1, z+1/2; (v) −x, y, −z+1/2.

Table S3. Selected single crystal X-ray diffraction pattern of **1** and **2** at 100 K showing that both crystals are stable during the data collection. The diffraction patterns of the same frame ($\omega$ = 0°, $\varphi$ = 0°) and the intensity of the same reflection (labeled with blue arrow) remain unchanged after ~24 h. The crystals of **1** and **2** are not stable under ambient conditions, losing crystallinity within hours of isolation from their mother liquors.

| | T (K) | 1st frame ($\omega$ = 0°, $\varphi$ = 0°) | 50th frame, ~0.5 h ($\omega$ = 0°, $\varphi$ = 15°) | 600th frame, ~6 h ($\omega$ = 0°, $\varphi$ = 180°) | 1st frame_2nd, ~24 h ($\omega$ = 0°, $\varphi$ = 0°) |
|---|---|---|---|---|---|
| **1** | 100 | 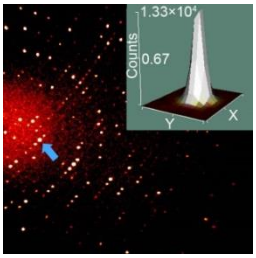  | 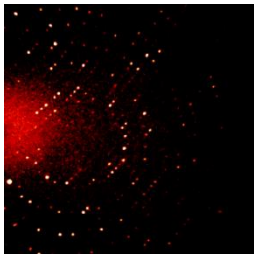 | 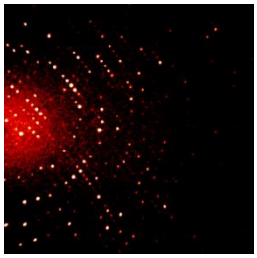 | 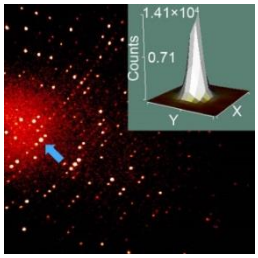  |
| | 300 | 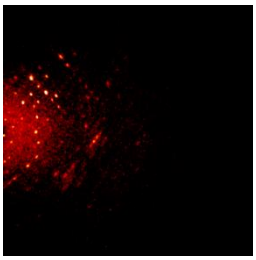 | 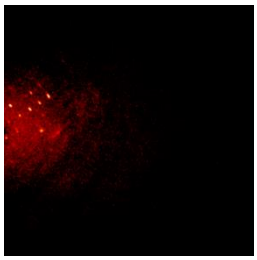 | 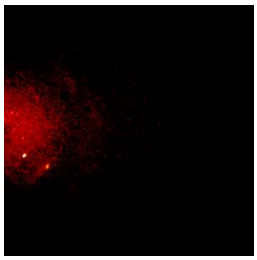 | |
| **2** | 100 | 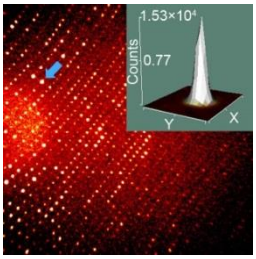  | 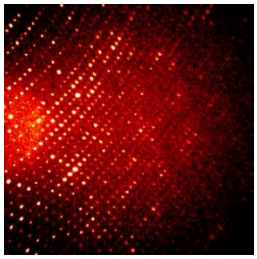 | 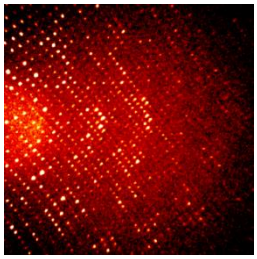 | 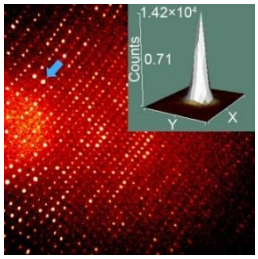  |
| | 300 | 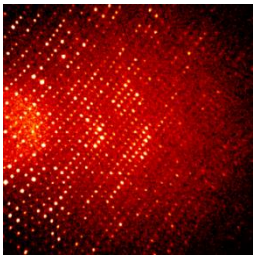 | 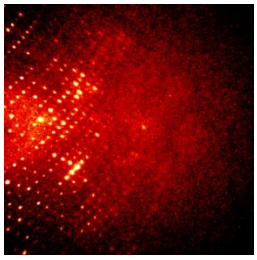 | 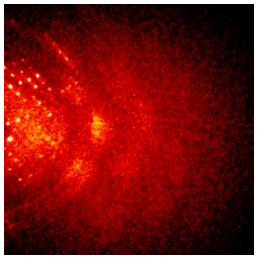 | |

## References


1. Knope, K. E.; Wilson, R. E.; Skanthakumar, S.; Soderholm, L., Synthesis and characterization of thorium(IV) sulfates. *Inorg. Chem.* **2011,** *50* (17), 8621-8629.
2. *Bruker APEX2 Software Suite, APEX2 v2011.4 –1; Bruker AXS: Madison, WI, 2011*.
3. *SMART, version 5.054; SAINT-Plus, version 6.45a; Bruker AXS: Madison, WI, 2003.*
4. Sheldrick, G., A short history of SHELX. *Acta Crystallogr., Sect. A* **2008,** *64* (1), 112-122.
5. Brese, N. E.; O'Keeffe, M., Bond-valence parameters for solids. *Acta Crystallogr. Sect. B* **1991,** *47* (2), 192-197.
6. Spek, A., PLATON SQUEEZE: a tool for the calculation of the disordered solvent contribution to the calculated structure factors. *Acta Crystallogr., Sect. C* **2015,** *71* (1), 9-18.
7. Albrecht, A. J.; Sigmon, G. E.; Moore-Shay, L.; Wei, R.; Dawes, C.; Szymanowski, J.; Burns, P. C., The crystal chemistry of four thorium sulfates. *J. Solid State Chem.* **2011,** *184* (7), 1591-1597.
8. Ben Mabrouk, K.; Kauffmann, T. H.; Aroui, H.; Fontana, M. D., Raman study of cation effect on sulfate vibration modes in solid state and in aqueous solutions. *J. Raman Spectrosc.* **2013,** *44* (11), 1603-1608.
9. Wilson, R. E.; Skanthakumar, S.; Knope, K. E.; Cahill, C. L.; Soderholm, L., An open-framework thorium sulfate hydrate with 11.5 Å voids. *Inorg. Chem.* **2008,** *47* (20), 9321-9326.